

Mechanical and Barrier Properties of Poly(lactic acid) Films Coated by Nanoclay-Ink Composition

Hyun Kyung Kim,¹ Seong Jin Kim,² Hyun Soo Lee,³ Jae Hoon Choi,³ Chang Myeong Jeong,³ Myoung Hwan Sung,³ Seok-Hoon Park,⁴ Hyun Jin Park^{4,5}

¹Korea Food Research Institute, 516 Baekhyundong Bungdanggu Songnamsi, Kyunggido 466-746, Republic of Korea

²CJ Cheil Jedang Food F&D Package Development Center, CJ CjeilJedang Corporation, Jungnim-Dong Jung-Gu, Seoul 100-791, Republic of Korea

³Research Development Department, Lotte Aluminum, 1005 Doksan-dong, Geumcheon-Gu, Seoul 153-010, Republic of Korea

⁴College of Life Sciences and Biotechnology, Korea University, Anam-Dong, Sungbuk-Ku, Seoul 136-701, Republic of Korea

⁵Department of Packaging Science, Clemson University, Clemson, South Carolina 29634-0320

H. K. Kim has contributed to this research as first author and both S.-H. Park and H. J. Park have equally contributed to this research as corresponding authors

Correspondence to: H. J. Park (E-mail: hjpark@korea.ac.kr)

ABSTRACT: In this study, poly(lactic acid) (PLA) films were coated by an ink formulation containing nanoclay dispersed with ultrasonic homogenization for 20 min. Mechanical and barrier properties of the coated films were evaluated according to clay type and concentration. PLA films coated by ink formulations containing Cloisite 30B displayed the best mechanical and barrier properties in six types of nanoclays. PLA films coated by Cloisite 30B-containing ink varying in clay concentration were investigated. Tensile strength and elongation at break of these coated films were improved in 1% Cloisite 30B. Oxygen permeability decreased significantly upon the addition of clay levels up to 1% and slightly decreased with further increases in the amount of the clay. The value of water vapor permeability also decreased depending on the increases of clay (0%–20%). When the clay content in the sample was 2.0%, the surface of coated PLA films displayed aggregation visible using film emission scanning electron microscopy. X-ray diffractometry and transmission electron microscopy indicated that a mixture of exfoliated and intercalated structure was formed with addition of 1% (w/w) Cloisite 30B to the ink after ultrasonication. © 2012 Wiley Periodicals, Inc. *J. Appl. Polym. Sci.* 000: 000–000, 2012

KEYWORDS: mechanical properties; barrier; films; coatings; clay

Received 29 November 2011; revised 6 February 2012; accepted 8 March 2012; published online 00 Month 2012

DOI: 10.1002/app.37663

INTRODUCTION

Growing dependence on synthetic plastic polymers has been one of the causes of global warming. These plastic wastes produce carbon dioxide that, when disseminated into the atmosphere, fuels atmospheric warming on the global scale. As well, there is a terrestrial concern, because most synthetic polymers are nonbiodegradable.¹ Therefore, biodegradable polymers have been evaluated as an alternative to synthetic materials.

Among the various biodegradable materials, poly(lactic acid) (PLA) is a useful natural biopolymer. PLA is a member of the family of aliphatic polyesters commonly made from lactic acid. PLA is synthesized from renewable resources such as corn and sugar beets via fermentation processes.² It is a thermoplastic,

high-strength, high-modulus polymer and is considered biodegradable and compostable.³ But, PLA has not been used extensively because the cost of production is higher and its applications more onerous than other petroleum-based commercial resins. As far as PLA availability in the market is concerned, PLA can be quenched into a quasi-amorphous state and crystallized upon annealing and orientation, because it is a slow crystallizing polymer like polyethylene terephthalate.⁴ The properties of thin PLA films prepared by a biaxial stretching method are superior to films made by blown or nonoriented methods.⁵ However, the pure PLA biopolymer exhibits low barrier properties and brittleness, which are disadvantages for food packaging applications.⁶ To overcome these limitations, nanocomposite technology has been applied to biopolymer films to enhance the barrier and mechanical properties.⁷

Nanoclays have become an attractive class of organic–inorganic hybrid materials because of their potential use in a wide range of applications such as polymer nanocomposites; rheological modifier in paints, inks, and greases and as a drug delivery carrier.⁸ Montmorillonite (MMT) is widely used in polymer nanocomposites. It is constructed of repeating triple-layer sheets composed of two tetrahedral silica sheets fused to an edge-shared octahedral sheet of alumina with a thickness of approximately 1 nm and a length of approximately 100 to several hundred nanometers. Stacking of the layers creates a gap between the layers called the interlayer or gallery.⁹

Gas barrier properties can be improved by addition of a coat. Coatings and printings provide the potential to control the transport of moisture, oxygen, aroma, oil, and flavor compounds in food systems, depending on the nature of the edible film-forming materials.^{10,11} For example, gravure printing is often used for high-volume printing of packaging, wallpaper, and gift wrap using fast-drying inks. A thin film, such as a PLA film, is generally coated by gravure ink for commercial use.

The main objective of this research was to prepare ink compositions incorporating several nanoclays and investigate the effect of the various ink composition coatings on the mechanical and barrier properties of PLA films. Additionally, various properties of PLA films coated by the ink composition were determined, depending on the nanoclay contents.

MATERIALS AND METHODS

Materials

PLA films of 20- μm thickness were supplied by SKC (Seoul, South Korea). Five organically modified and one pristine MMT clay were purchased from Southern Clay Products (Austin, TX). The modified MMTs were Cloisite 20A (dimethyl dehydrogenated tallow quaternary ammonium-MMT, 95 mequiv/100 g clay), Cloisite 25A (dimethyl dehydrogenated tallow 2-ethylhexyl quaternary ammonium-MMT, 95 mequiv/100 g clay), Cloisite 30B (methyl tallow bis-2-hydroxyethyl quaternary ammonium-MMT, 90 mequiv/100 g clay), and Cloisite 93A (methyl dehydrogenated tallow ammonium-MMT, 90 mequiv/100 g clay). The unmodified MMT was Cloisite Na+ [cation exchange capacity 1/4 92 mequiv/100 g clay]. Gravure ink (TiO₂, Poly Vinyl Copolymer, Poly Urethane, Additives) that was with transparent and a solvent composed of methyl ethyl ketone and ethyl acetate were supplied by IPC (Seoul, South Korea).

Preparation of Nanoclay–Ink Formulations

Ink solutions were made by mixing the aforementioned ink and solvent at a 1 : 1 ratio (v/v) and vigorously stirring for 1 h. Various amounts of nanoclay (0%–2.0% by weight) were added and mixing vigorously by magnetic stirring for 30 min followed by ultrasonic homogenization for 20 min to obtain the final ink–nanoclay formulations.

Film Coating with the Nanoclay–Ink Formulations

Each ink–nanoclay formulation was coated on PLA films using a Model 542-AB automatic film applicator (Yasuda Seiki Seisakusho, Hyogo, Japan) operating at 300 mm/s and a coating speed of 60 Hz. The coated PLA films were dried at ambient conditions for 24 h. All film samples were then preconditioned for at least 48 h in a constant temperature humidity chamber set at 25°C and 50% rela-

tive humidity before testing. The thickness of coating layer in PLA films coated by ink composition with 0% and 1% Cloisite 30B were 1.42 and 1.44, respectively. When it comes to commercial thickness of coating layer, from 1.5 to 2.0 μm is suitable.

Mechanical Properties

The tensile strength (TS) and elongation (E) at break were measured with a Model 5566 Universal Testing Machine (Instron, Canton, MA). All specimens were 10 cm \times 2.54 cm in size. Initial grip separation and cross-head speed were set at 5 cm and 500 mm/min, respectively. TS was calculated by dividing the maximum load (N) by the initial cross-sectional area (m^2) of the specimen. E was calculated and expressed as the percentage of change of the original length of a specimen between grips (5 cm). Each test was replicated at least five times for each type of film.

Oxygen Permeability

An OX-TRAN Model 2/61 (Mocon, Minneapolis, MN) was used for the measurements. Oxygen gas (100%) was flowed over the coated side of the film. Nitrogen gas (98% nitrogen, 2% hydrogen) was flowed over the opposite surface. Testing was performed at 23°C at a relative humidity of 0% and done in triplicate to get the average mean value. Oxygen permeability (OP) ($\text{cc m/m}^2 \text{ day atm}$) was calculated by multiplying the oxygen transmission rate by the film thickness.

Water Vapor Permeability

The water vapor permeability (WVP) of films was determined gravimetrically based on ASTM (E96-80) procedure modified for the vapor pressure at the underside film. Samples were 7 cm \times 7 cm in size. The test films were sealed to cups containing distilled water and placed in a Model TR-001-1 constant temperature and humidity chamber at 25°C and 50% relative humidity (Jeio Tech, Seoul, Korea). Weight loss was measured at 2 h intervals for 12 h. The slopes were calculated by linear regression and correlation coefficients for all reported data were >0.99 . The measurement (WVP) was calculated as follows:

$$\text{WVP} = (\text{WVTR} \times L) / \Delta P \quad (1)$$

where WVTR is the measured water vapor transmission rate ($\text{g/m}^2 \text{ s}$) through the film, L is the mean film thickness (m), and ΔP is the partial water vapor pressure difference (Pa) across the two sides of the film.

Field Emission Scanning Electron Microscopy

Morphology of the surface of films and liquid nitrogen freeze-fractured cross-sections of films were visualized using a MIRA II field emission scanning electron microscopy (FE-SEM) (TESCAN, Brno, Czech Republic) at an acceleration voltage of 5.0 kV.

X-ray Diffraction

X-ray diffraction (XRD) patterns of film samples were obtained by small-angle X-ray scattering using a General Area Detector Diffraction System (Bruker AXS, Madison, WI). The area detector operated at a voltage of 40 kV and a current of 45 mA with Cu-K α radiation ($\lambda = 0.15406 \text{ nm}$). According to the Bragg equation, the gap between silicate layers (d_{001}) can be calculated as follows:

$$n\lambda = 2d \sin \theta, \quad (2)$$

where $n = 1$, λ (wavelength of X-ray radiation) = 1.54056 Å, d = spacing distance between the diffracting layers, and θ = grazing

Table I. TS and %E of PLA Films Coated by Nanoclay-Ink Formulations with Different Clay Types

| PLA film | TS (MPa) | E (%) |
|--|---------------------------|-------------------------|
| Neat PLA | 78.9 ± 5.4 ¹ | 14.7 ± 2.7 ² |
| Control ^a | 79.1 ± 5.8 ¹ | 14.3 ± 3.8 ³ |
| coated by ink composition/Cloisite Na | 84.9 ± 2.4 ³ | 17.8 ± 1.9 ¹ |
| coated by ink composition/Cloisite 20A | 81.3 ± 4.2 ^{2,3} | 32.1 ± 3.1 ² |
| coated by ink composition/Cloisite 25A | 88.5 ± 2.3 ³ | 31.0 ± 2.5 ² |
| coated by ink composition/Cloisite 30B | 92.9 ± 2.1 ² | 12.2 ± 1.0 ⁴ |
| coated by ink composition/Cloisite 93A | 81.2 ± 1.7 ³ | 30.2 ± 5.9 ² |

Same superscript numeral within a column indicate no significant ($P > 0.05$) difference by Duncan multiple range test.

^aCoated chitosan film by ink composition with only ink.

angle of the incident wave. This equation can be applied when the XRD angle is small.

Transmission Electron Microscopy

Ultrathin films (120 nm) for transmission electron microscopy (TEM) observation were prepared by cutting the coated PLA film sheet at room temperature using an ultramicrotome (Leica, Wetlar, Germany). The films were collected in a water-filled trough and placed on 200-mesh copper grids. Coated PLA film samples were cross-linked in 50% glutaraldehyde before being cut to retard the dissolution of the ultrathin films in the water trough. TEM was done using a Tecnai G2 Spirit transmission electron microscope (FEI, Hillsboro, OR) at an accelerating voltage of 120.0 kV.

Table II. TS and %E of PLA Films Coated by Nanoclay-Ink Formulations with Different Clay Contents

| PLA film | TS (MPa) | E (%) |
|---|---------------------------|-------------------------|
| Coated by ink composition/0% Cloisite 30B | 79.1 ± 5.8 ¹ | 14.3 ± 3.8 ² |
| Coated by ink composition/0.5% Cloisite 30B | 91.3 ± 5.5 ² | 7.9 ± 1.2 ¹ |
| Coated by ink composition/1.0% Cloisite 30B | 92.9 ± 2.1 ² | 5.5 ± 0.8 ¹ |
| Coated by ink composition/1.5% Cloisite 30B | 91.0 ± 7.0 ² | 7.2 ± 1.8 ¹ |
| Coated by ink composition/2.0% Cloisite 30B | 86.7 ± 2.0 ^{1,2} | 12.2 ± 2.4 ² |

Same superscript numeral within a column indicate no significant ($P > 0.05$) difference by Duncan multiple range test.

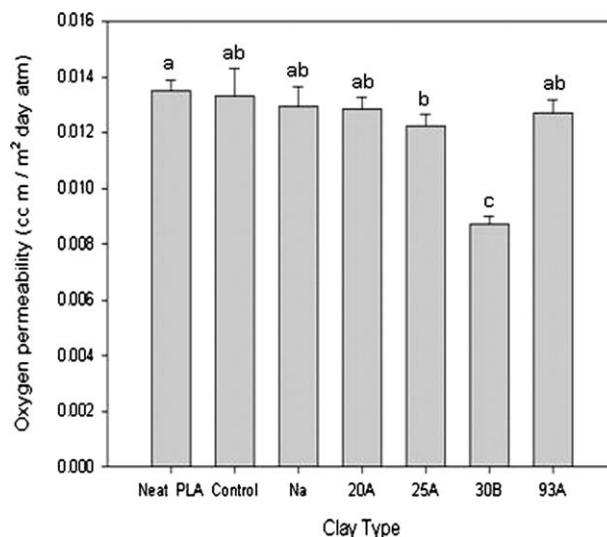


Figure 1. OP of PLA films coated by ink formulations with different clay types.

Statistical Analysis

Data were analyzed using SAS software version 9.1 (SAS Institute, Cary, NC). Duncan's method was used for multiple mean comparisons among treatments at $\alpha = 0.05$. One replication based on analysis on three samples was tested; the reported values represent the mean ± standard error.

RESULTS AND DISCUSSION

Mechanical Properties

Effect of Nanoclay Type. The TS and elongation (E) at break are able to describe how the mechanical properties of film materials are related to their chemical structure.¹² The mechanical properties of PLA films coated by the ink formulations as a function of clay type are presented in Table I. The TS value of each control film was increased compared with the neat biopolymer films. The strengthening effect of the coating can be attributed to the constrained effect of the film.¹³ The TS value

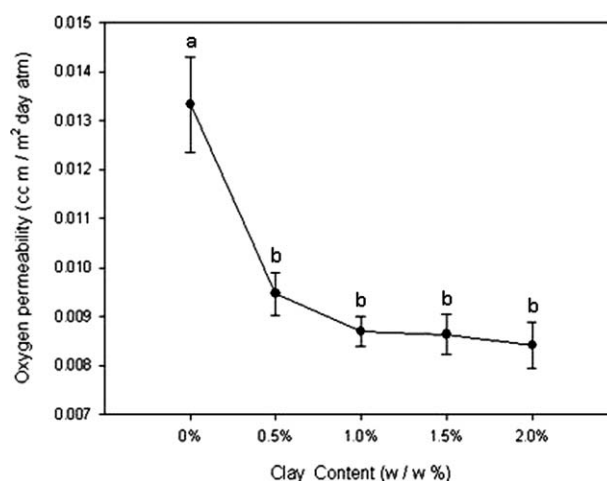


Figure 2. OP of PLA films coated by ink formulations with different clay types.

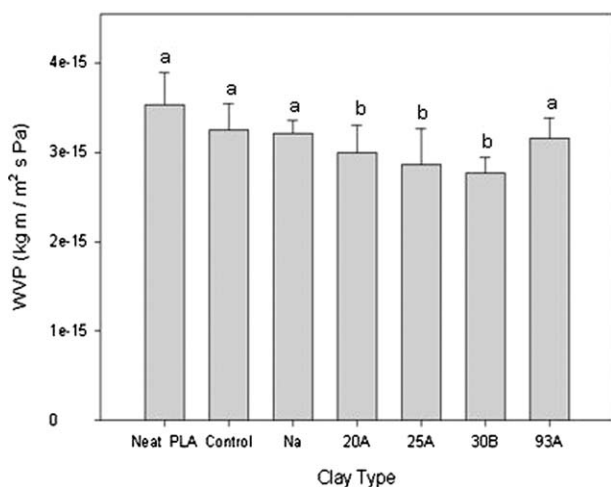


Figure 3. WVP of PLA films coated by ink formulations with different clay types.

of PLA films coated by nanoclay containing ink was 3%–17% better compared with control PLA films. Among the other clay types, PLA films coated with Cloisite 30B containing ink displayed the highest TS and lowest E , indicating that Cloisite 30B might have the best dispersion in the matrix, because the extent of the increase in TS depends directly upon the average length of the dispersed clay particles.¹⁴

Effect of Nanoclay Content. Table II summarizes the data concerning the effect of clay content on TS and E of PLA films coated by Cloisite 30B containing ink. The tensile properties of all the coated PLA films were significantly increased compared with control films. Such a reinforcing effect on biopolymer films as a result of the presence of a nanoparticle containing coat can be mainly attributed to a possible strain-induced alignment of the nanoparticle layers in the matrix.¹⁵ The TS of PLA

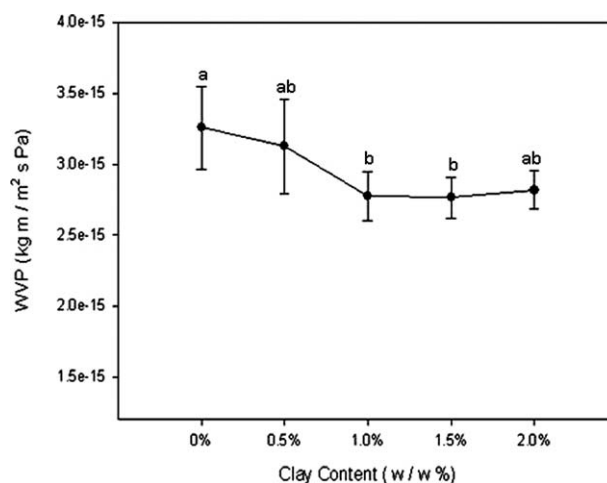


Figure 4. WVP of PLA films coated by ink formulations with different clay contents.

films coated by Cloisite 30B containing ink formulations increased significantly with increasing amount of Cloisite 30B up to 1% (w/w), followed by a decrease with a further increase in Cloisite 30B up to 2% (w/w). This enhancement of TS with the addition of a low content of Cloisite 30B can be ascribed to the formation of an intercalated or exfoliated state, and the uniform dispersion of clay in the matrix.¹⁶ However, when the clay content increases, Cloisite 30B aggregates easily and the intercalation or exfoliation of the ink composition becomes difficult.¹⁷

Oxygen Barrier Properties

Effect of Clay Type. The effect of nanoclay type on the OP of the PLA films coated by the various ink formulations is shown in Figure 1. The OP value of neat biopolymer films and control biopolymer films (coated only by ink) showed significant differences, consistent with the idea that coating retards the molecular diffusion of oxygen.¹⁸ The OP value of the PLA films coated

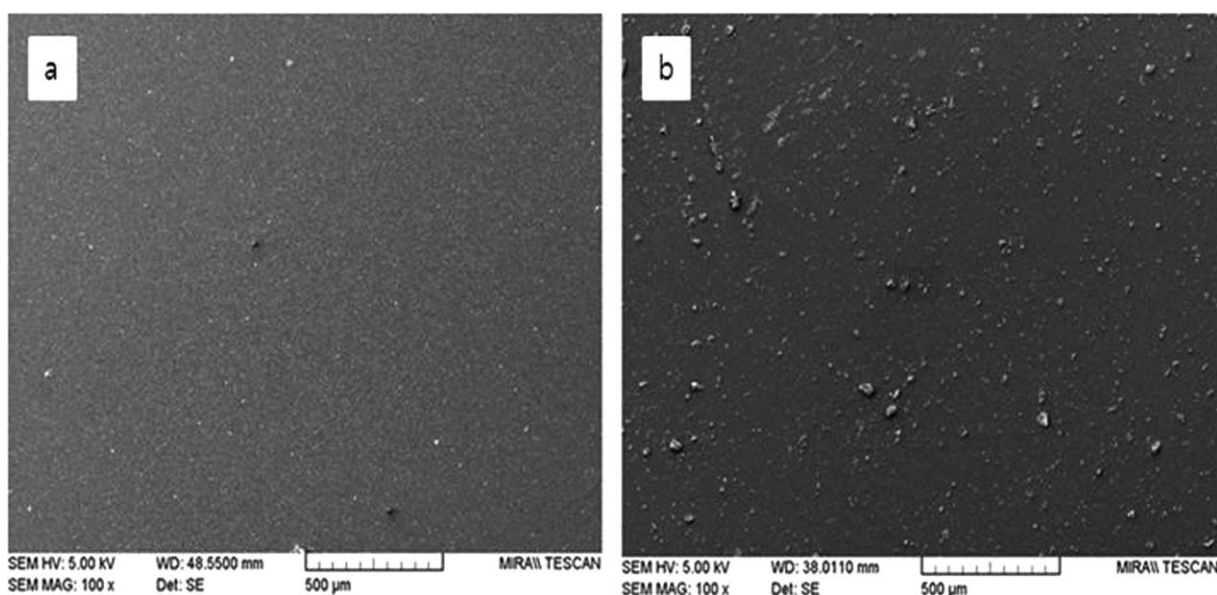


Figure 5. Surface micrographs of PLA films coated by ink formulations containing (a) Cloisite 30B and (b) Cloisite Na⁺.

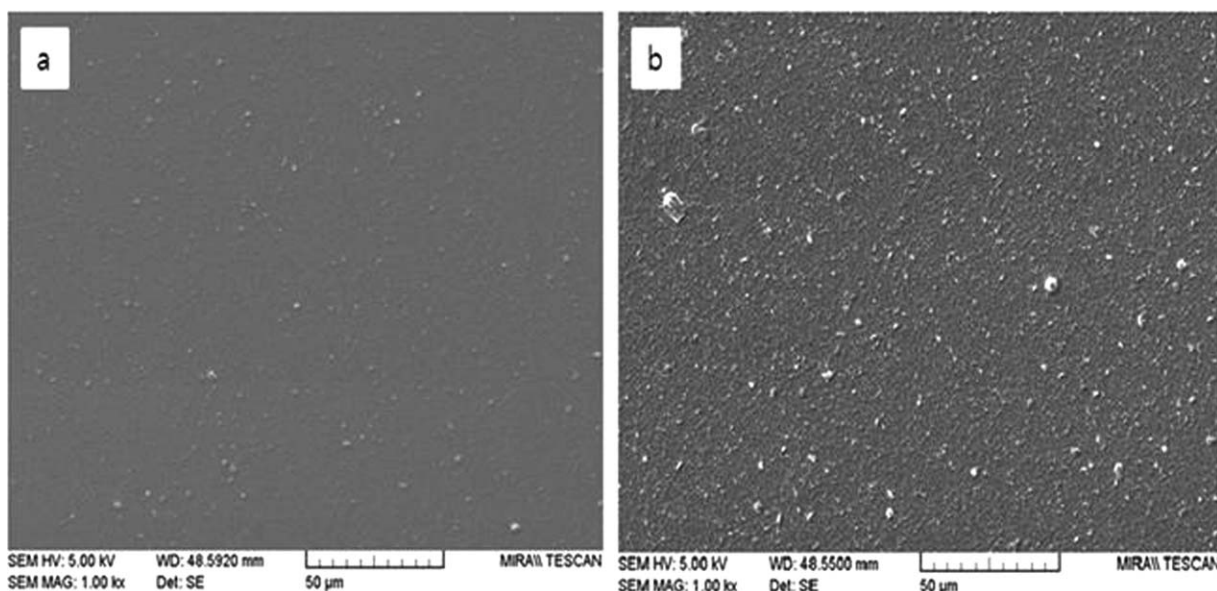


Figure 6. Surface micrographs of PLA films coated by ink formulations with (a) 1% (w/w) Cloisite 30B and (b) 2% (w/w) Cloisite 30B.

by ink formulations containing unmodified MMT (Cloisite Na⁺) was slightly higher compared with ink containing modified MMT (Cloisite 20A, Cloisite 25A, Cloisite 30B, and Cloisite 93A). A previous study reported that the incomplete dispersion of the nanoclay into the polymer matrix is caused by the incompatibility of hydrophobic nanoclay with hydrophilic polymer.¹⁹ In this case, it was mainly attributed incomplete dispersion between the hydrophilic character of Cloisite Na⁺ and the hydrophobic character of the ink solution.¹⁹ On the other hand, presently, Cloisite 30B was the lowest OP value of PLA film coated by ink composition in the five types of modified MMT, given that Cloisite 30B is more ink compatible.

Effect of Clay Content. Figure 2 displays the OP of PLA films coated by ink formulations containing different amounts of Cloisite 30B. The OP value of PLA films significantly decreased to 1% (w/w) of clay content. This improved gas barrier performance resulting from the impermeable clay layers forces a tortuous pathway for a traversing permeant.²⁰ However, pres-

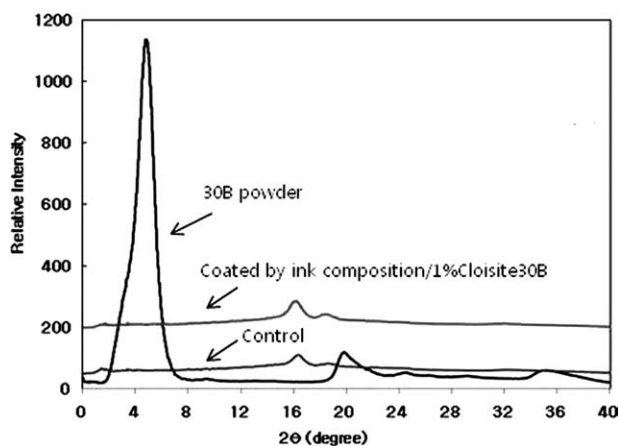


Figure 7. XRD patterns of Cloisite 30B, a neat PLA film and a PLA film coated by ink formulated with 1% (w/w) Cloisite 30B.

ently, there was no statistically evident difference with a further increase up to 2% (w/w) of clay content. Considering practical and economical uses, an ink formulation containing 1% (w/w) of clay is considered appropriate.

Water Vapor Barrier Properties

Effect of Clay Type. WVP values of the PLA films coated by ink composition with different type of clay are summarized in Figure 3. One of the disadvantages of biopolymer films is poor water vapor barrier property.¹¹ Compared with neat biopolymer films, the control biopolymer films (i.e., those coated only by ink) presently displayed a markedly lower WVP value due to the coating layer. PLA film coated with Cloisite containing ink displayed the lowest WVP. The increase in water vapor barrier property may also have been due to the development of compatibility between the ink solution and the nanoparticles. Therefore, this good dispersion may increase the effective path length for water vapor diffusion.

Effect of Clay Content. Figure 4 displays the effect of clay content on WVP of PLA films coated by Cloisite 30B containing ink. The addition of clay significantly enhanced the water vapor barrier properties of these films. The decrease in WVP is believed to be due to the presence of ordered dispersed nanoparticle layers with large aspect ratios in the matrix, which forces water vapor traveling through the film to follow a tortuous path through the matrix surrounding the nanoparticles, thereby increasing the effective path length for diffusion.^{21,22} The influence of clay concentration on WVP depends on the type of composition formed (tactoids, intercalation, and exfoliation). Intercalation and exfoliation are two ideal nanoscale compositions, the formation of which depends on the types and amounts of nanoclay used.²³

FE-SEM

Figure 5 depicts the FE-SEM observations of PLA films coated by ink formulations containing two different types of nanoclays.

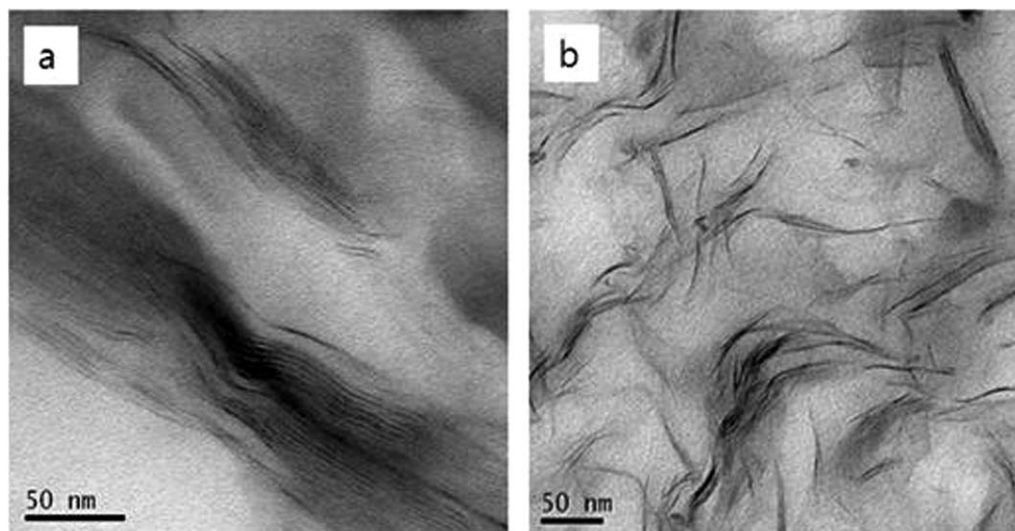


Figure 8. TEM of PLM films coated with ink containing 1% Cloisite 30B. (a) No dispersion time. (b) Dispersion time of 20 min.

Figure 5(A) shows the typical appearance of films containing modified MMT (Cloisite 30B) and Figure 5(B) shows the typical appearance of films containing unmodified MMT (Cloisite Na⁺). The latter films displayed markedly bigger particles and some aggregations, indicating the superior dispersion capability of modified MMT (Cloisite 30B) in the ink formulations.

Figure 6 shows the results obtained with PLA films coated by the ink formulations. The surface of PLA films coated by ink formulated with 1% Cloisite 30B was smooth [Figure 6(a)], whereas film coated with ink containing 2% Cloisite 30B produced a rough surface [Figure 6(b)]. The difference is likely due to the disparate dispersibility between these nanoclays and the ink solution.

XRD

XRD is a classical method for determining the gallery height (d -spacing distance) in clay particles.²⁴ During intercalation or exfoliation, d -spacing increases and the diffraction peak shifts lower angles. Presently, the assessment of the dispersion of the clays in the ink formulations was done using XRD (Figure 7). The XRD patterns of the Cloisite 30B powder displayed a silicate reflection at $2\theta = 4.82^\circ$, indicative of an increased d -spacing distance compared with that of unmodified MMT due to the replacement of sodium ions with quaternary ammonium cations.¹⁴ The XRD result of PLA films coated by 1% Cloisite 30B containing displayed the same pattern as control biopolymer films that were coated only by ink. The reflection peak of Cloisite 30B powder disappeared. This suggests the occurrence of exfoliation. Similarly, a previous study reported that in the exfoliated state, the diffraction from the clay interlayer spacing disappears.²⁵

TEM

It is difficult to make any definitive conclusions about structure using the XRD result alone.²⁶ Therefore, TEM is used to determine the internal structure, spatial distribution of the various phase and views of the defect structure through direct visualization.^{1,27} Figure 8 shows a representative TEM photograph of a

PLA film coated by an ink formulation containing 1% Cloisite 30B with different dispersion times. In the coating layer, the dark line represents the cross-section of an individual clay layer. The gap between the two adjacent layers is the interlayer spacing or gallery. As can be seen in the Figure 8(a), large agglomerates were clearly visible, along with tactoids of silicates in the samples. However, the clays were mostly exfoliated and some were intercalated in the coating layer [Figure 8(b)]. The dimensions of the dispersed clay particles were quite fine, and their spatial distribution was homogeneous. Combining the results of TEM and XRD, the coexistence of an exfoliated-intercalated clay structure is indicated.

CONCLUSION

In this research, PLA films coated by clay containing ink formulations displayed improved mechanical and barrier properties compared with PLA films coated only by ink. Cloisite 30B enhanced the barrier and mechanical properties among the five types of nanoclays. This result indicates that Cloisite 30B is more effectively dispersed in ink solutions. A nanoclay content of 1% also improved the mechanical and barrier properties of PLA films coated by nanoclay-ink formulations. These results depend on the dispersibility of nanoclay in the gravure ink solution. TEM and XRD analyses indicated that exfoliation, along with some intercalation, occurred in PLA films coated by an ink formulation containing 1% (w/w) Cloisite 30B after ultrasonication. Therefore, PLA films coated by nanoclay containing ink formulations have great potential for application in food packaging to improve mechanical and barrier properties.

REFERENCES

- Okamoto, M. *J. Ind. Eng. Chem.* **2004**, *1*, 1.
- Garlotta, D. *J. Polym. Environ.* **2001**, *9*, 63.
- Jararat, A.; Tokiwa, Y. *Macromol. Biosci.* **2001**, *1*, 136.
- Ou, X.; Cakmak, M. *Polymer* **2008**, *49*, 5344.

5. Lim, L. T.; Auras, R.; Rubino, M. *Prog. Polym. Sci.* **2008**, *33*, 820.
6. Cabedo, L.; Feijoo, J. L.; Villanueva, M. P.; Lagaron, J. M.; Gimenez, E. *Macromol. Symp.* **2006**, *233*, 191.
7. Kim, J. T.; Lee, D. Y.; Lee, T. S.; Lee, D. H. *J. Appl. Polym. Sci.* **2003**, *89*, 2633.
8. Patel, H. A.; Somani, R. S.; Bajaj, H. C.; Jasra, R. V. *Bull. Mater. Sci.* **2006**, *29*, 133.
9. Alexandre, M.; Dubois, P. *Mater. Sci. Eng. Rep.* **2000**, *28*, 1.
10. Donhowe, G.; Fennema, O. *J. AOCS* **1993**, *70*, 867.
11. Krochta, J. M.; De, M. C. *Food Technol.* **1997**, *51*, 61.
12. Ninnemann, K. W. Measurement of Physical Properties of Flexible Films. The Science and Technology of Polymer Films. Interscience: London, England, **1968**; Vol.13, p 546.
13. Ochiai, S.; Murakami, Y. *Met. Sci.* **1976**, *10*, 401.
14. Rhim, J. W.; Hong, S. I.; Park, H. M.; Perry, K. W. *J. Agric. Food Chem.* **2006**, *54*, 5814.
15. Giannelis, E. P. *Adv. Mater* **1996**, *8*, 29.
16. Zheng, J. P.; Li, P.; Ma, Y. L.; Yao, K. D. *J. Appl. Polym. Sci.* **2002**, *86*, 1189.
17. Zhang, Q.; Qiang, F.; Luxia, J.; Yong, L. *Polym. Int.* **2000**, *49*, 1561.
18. Hammon, H. G.; Ernst, K.; Newton, J. C. *J. Appl. Polym. Sci.* **1997**, *21*, 1989.
19. Sothornvit, R.; Rhim, J. W.; Hong, S. I. *J. Food. Eng.* **2009**, *91*, 468.
20. LeBaron, C. P.; Zhen, W.; Pinnavaia, T. *J. Appl. Clay Sci.* **1999**, *15*, 11.
21. Yano, K.; Usuki, A.; Okad, A. *J. Polym. Sci. Part A: Polym. Chem.* **1997**, *35*, 2289.
22. Cussler, E. L.; Highes, S. E.; Ward, W. J.; Aris, R. *J. Membr. Sci.* **1998**, *38*, 161.
23. Xu, Y.; Ren, X.; Hanna, M. A. *J. Appl. Polym. Sci.* **2006**, *99*, 1684.
24. Di, Y. W.; Iannace, S.; Maio, E. D.; Nicolais, L. *J. Polym. Sci. Part B: Polym. Phys.* **2003**, *41*, 670.
25. Rao, Y. *Polymer* **2007**, *48*, 5369.
26. Wang, S. F.; Shen, L.; Tong, Y. J.; Chen, L.; Phang, I. Y.; Lim, P. Q.; Liu, T. X. *Polym. Degrad. Stab.* **2005**, *90*, 123.
27. Sinha Ray, S.; Okamoto, M. *Prog. Polym. Sci.* **2003**, *28*, 1539.